# A METHODOLOGY FOR MODELING THE DISTRIBUTION OF TURNING VEHICLE PATHS AT SIGNALIZED INTERSECTIONS


Wael K. M. Alhajyaseen
Dr. Eng., Postdoctoral Research Fellow, Department of Civil Engineering, Nagoya University, Furo-cho, Chikusa-ku, Nagoya 464-8603, Japan, e-mail: wael@genv.nagoya-u.ac.jp

Miho Asano
Dr. Eng., Assistant Professor, Department of Civil Engineering, Nagoya University, Furo-cho, Chikusa-ku, Nagoya 464-8603, Japan, e-mail: asano@genv.nagoya-u.ac.jp

Hideki Nakamura
Dr. Eng., Professor, Department of Civil Engineering, Nagoya University, Furo-cho, Chikusa-ku, Nagoya 464-8603, Japan, e-mail: nakamura@genv.nagoya-u.ac.jp

Dang Minh Tan
M.Sc., Doctor candidate, Department of Civil Engineering, Nagoya University, Furo-cho, Chikusa-ku, Nagoya 464-8603, Japan, e-mail: dang@genv.nagoya-u.ac.jp



*Submitted to the 3rd International Conference on Road Safety and Simulation, September 14-16, 2011, Indianapolis, USA*


## ABSTRACT


Analytical evaluation approaches for the safety performance of signalized intersections are applicable for limited scenarios and conditions; whereas simulation based analysis tools are very flexible and promising. This study is a part of intensive efforts to develop a microscopic simulation model for the safety assessment of signalized intersections. One of the important aspects in analyzing driver maneuver, which has vital impacts on the safety performance of signalized intersections, is vehicle paths. Broadly varying paths may result in widely distributed conflict points with other conflicting movements which may affect the occurrence probability of severe conflicts. Therefore, this paper aims to develop a methodology to reproduce the variations in the paths of turning vehicles (right-turning and left-turning) considering intersection geometry, vehicle type and speed. Several signalized intersections in Nagoya City, Japan with various traffic and geometric characteristics were videotaped. A pre-developed video image processing system TrafficAnalyzer (Suzuki and Nakamura, 2006) is utilized to extract vehicle maneuvers. The analysis revealed that the paths of right-turning vehicles are more sensitive to vehicle speed and turning angle while those of left-turning vehicles are more sensitive to intersection corner radius, turning angle and vehicle speed. For modeling individual vehicle paths, this paper applies the Euler-spiral-based approximation methodology where each trajectory is fitted by an entering Euler spiral curve followed by a circular curve and an exit Euler spiral curve. The proposed

models are unique since they provide a realistic and rational representation of the variations in turning vehicles' paths inside intersections.

**Keywords:** intersection geometry, turning vehicles, vehicle path, Euler spiral curve, simulation

## INTRODUCTION

Depending on the cultural customs, prevailing traffic characteristics and available technologies locally, various safety improvements are implemented at intersections, however they are so far based on experience and after implementation assessments. A major achievement would be to enable engineers to conduct before implementation assessments at the planning stage. Simulation tools are the means to realize such an assessment. Existing simulation software, however, simplifies the traffic flow inside intersections to an extent that safety assessments are not reliable.

This study is a part of continuous efforts for developing a microscopic simulation model for the safety assessment of signalized intersections. This model would allow practitioners to evaluate the effects of various improvements in the layout and operation of signalized intersections on the overall safety performance. For instance, through this simulation, it would be possible to predict the impacts of adding channelization or adjusting the positions of crosswalks or intersection corner radii. And it can further be applied to modify the signal timing parameters such as all-red intervals. However in order to develop such a rational simulation model, driver behavior must be reasonably reflected in it.

One of the important aspects in analyzing driver behavior, which is a vital element in the safety performance of signalized intersections, is vehicle paths (spatial trajectories). Several existing studies found that there are significant variations in trajectories of turning vehicles. It is rational to assume that such variations might result in creating specific unfavorable conditions which might lead to collisions. In reality, road users behave by anticipating other users' behavior in order to avoid any collisions with them. Broadly varying road user behavior and trajectories may lead to misunderstanding of other users' decisions which might result in safety problems. Large variations in vehicle paths lead to widely distributed conflict points with other users. This indicates that users have to pay attention to a broader area where conflicts may occur. Therefore, it is quite important to consider not only average vehicle maneuver but also its variations which are affected by the geometric layout of intersections and the interaction with other users.

The paths of left-turning and right-turning vehicles (definition is based on left-hand traffic) have different characteristics and influencing factors. In common signal phasing plans, pedestrians and through-left turning traffic of the same direction share the same phase, thus left-turners will have frequent conflicts with pedestrians and cyclists, which might leave some effects on their paths whereas right- turning vehicles are often provided with exclusive phases which significantly limit the effects of pedestrians and cyclists. Furthermore, right-turning vehicles might be affected by various geometric elements since they cross from the middle of the intersection, for instance turning angle (the angle between entering and exit approaches) and median configuration at the entering and exiting approaches. Whereas it is expected that left-turning vehicles are affected by corner radius and turning angle.

The objective of this paper is to investigate influencing factors on turning vehicle paths and its variations. For this, a model which can represent the variations in turning vehicle paths (left-turning and right-turning) under different geometric conditions is proposed. Spatial distributions of vehicle paths are analyzed considering intersection geometries, vehicle types and the existence of pedestrians or cyclists. Finally this paper ends up with conclusions and future works.

## LITERATURE REVIEW

It is commonly assumed that the design vehicle turn templates such as the one showed in AASHTO (2004) provide actual turning paths. However, the variation in driver-vehicle interaction at intersections and the resulted paths has not been studied nor analyzed intensively.

Stover (2008) addressed the issue of the variations in vehicle turning trajectories as one of the main concerns that should be carefully studied in the design of intersections since a significant variation in driver paths was found empirically. Stover and Koepke (2002) presented a number of figures illustrating the dispersion of the paths of right-front wheel of right-turning vehicles (right-hand traffic) for various combinations of curb radii and driveway widths. These figures clearly showed a considerable variability in vehicle trajectories. However they did not provide any quantification for such variations.

Decabooter and Solberg (1988) collected data for several trucks making right-turn (right-hand traffic) at two signalized intersections. A camera system was used to obtain the observed paths of the left-front overhangs and the right-rear wheels of individual vehicles. They found significant variations in the paths of trucks in the two sites which reflect that drivers behave in different manners at the same intersection geometric characteristics. However they did not provide any methodologies to predict such kind of variations under various geometric and traffic conditions.

Read (2008) analyzed the effect of vehicles body (A-pillar) on driver visibility and its effect on the variation in the paths of right and left turning vehicles. However since the objective of their study was toward vehicle design issues, they did not go deeply in modeling and analyzing the factors that affect driver behavior while turning.

Although these studies analyze the variations in the paths of vehicles, they have not yet quantitatively analyzed how intersection geometric characteristics affect on paths and their variation. This paper proposes an empirical model to explain this relationship.

Asano, et al. (2011) analyzed the paths of left-turning vehicles (left-hand traffic) at several signalized intersection in Nagoya City, Japan. They analyzed the effect of intersection geometry on the variations of vehicle paths. They proposed a procedure to model the variations in left-turning vehicle paths. The modeling methodology is based on approximating individual vehicle paths using a polygonal line. The results showed that left-turning vehicle paths can be well fitted by using a polygonal line which is a combination of straight segments, Euler spiral curve segments and circular curve segments. One of the shortcomings of their proposed models is that they do not consider the effect of left-turning vehicle speed. Furthermore, their analysis is limited to left-turning vehicles.

Table 1 Surveyed sites for the analysis of left-turning paths

| Intersection name | Approach | Survey date | Radius of the corner $R_c$ (m) | Intersection angle (deg) | Number of exit lanes $N_o$ | Crosswalk setback Distance $D_s$ (m) |
|---|---|---|---|---|---|---|
| Suemori-dori 2 | East | 11/18/2008 9:00-12:00 | 9.7 | 88.3 | 2 | 4.8 |
| | West | | 19 | 65.4 | 2 | 8.3 |
| | North | | 17 | 117 | 3 | 13.1 |
| Chikatetsu Horita | East | 06/18/2009 9:00-10:30 | 14 | 94.1 | 3 | 3.5 |
| | South | | 12 | 88.3 | 3 | 13.7 |
| Taiko-dori 3 | West | 10/13/2009 7:30-10:30 | 17 | 94.1 | 3 | 12.4 |
| | South | | 17 | 88.3 | 2 | 14.6 |
| Nishi-osu | West | 01/18/2009 9:00-12:30 | 17 | 76.9 | 3 | 17.8 |
| Kawana | West | 12/01/2008 7:30-10:30 | 21 | 106 | 2 | 22.0 |
| Imaike | East | 10/15/2005 13:00-15:00 | 16 | 91.2 | 3 | 18.5 |

This paper is an extension to the previous works done by Asano, et al. (2011), aiming at refining the developed empirical models to consider vehicle speed and to extend the analysis to right-turning vehicles as well.

## STUDY SITES AND DATA OBSERVATION

### Study Sites

In order to analyze the significance of various influencing factors on the maneuver of turning vehicles (left-hand traffic), video data was collected at several signalized intersections with different geometric and traffic conditions. Table 1 and Table 2 present the observation dates and geometric characteristics of the observed sites for the analysis of left-turning vehicles and right-turning vehicles, respectively. All these sites are located in Nagoya City, Japan. The definitions of the parameters in Table 1 and Table 2 are illustrated in Figure 1. The observed sites have significantly different geometric layouts such as curb radii, intersection angles, crosswalk setback distances and median configurations. Such a wide range of layouts is necessary to rationally study the variations in the maneuver of turning vehicles. All observed sites in Table 2 are operated with an exclusive right-turning phase. Thus observed right turning vehicles have theoretically no conflict with opposite through traffic or crossing pedestrians.

The average turning vehicle, pedestrian and bicycle demands during the observation periods are presented in Table 3. Pedestrian and left-turning vehicle demands are quite high at Imaike Intersection. Furthermore, according to the observations all sites have very low left-turning heavy vehicle demands except Nishi-osu Intersection where almost 14% of the observed left-turning vehicles are heavy vehicles. Regarding right-turners, most of them are passenger cars at all observation sites.

Table 2 Surveyed sites for the analysis of right-turning paths

| Intersection name | Approach | Survey date | Number of exit lanes $N_o$ | Intersection angle $\theta_r$ (deg.) | Distance from center of the intersection * to the median hard nose ($m$): Entering hard nose | Distance from center of the intersection * to the median hard nose ($m$): Exiting hard nose |
|---|---|---|---|---|---|---|
| Suemori-dori 2 | West | 11/18/2008 9:00-12: 00 | 2 | 88 | 15.3** | 13.9 |
| | North | | 3 | 67 | 23.0 | 13.6** |
| | South | | 3 | 93 | 17.2 | 12.0 |
| Sunadabashi | West | 6/27/2008 7:30-11:00 | 2 | 90 | 19.3 | 18.5 |
| | North | | 2 | 91 | 15.3 | 19.1 |
| Nishi-osu | North | 01/18/2009 9:00-12:30 | 3 | 74 | 31.1 | 31.0 |
| | East | | 3 | 106 | 27.2 | 29.2 |
| Kawana | North | 12/01/2008 7:30-10:30 | 2 | 106 | 35.4 | 24.1 |
| Sakurayama | South | 12/04/2008 7:20-10:20 | 2 | 90 | 22.9 | 29.2 |
| Atsuta Shrine South | North | 12/04/2008 7:00-12:00 | 3 | 61 | 21.1 | 23.2 |
| Taiko-dori 3 | West | 10/31/2009 7:30-10:30 | 3 | 84 | 22.6 | 17.2 |
| | North | | 2 | 95 | 17.9 | 22.1 |

* Center of the intersection is defined as the crossing point of the median extension from the entering and exiting approaches.

**At the West approach of Suemori-dori 2 intersection, there is a plastic pole in the zebra marking after the hard nose of the median. Thus, this pole is considered as the hard nose of the median.

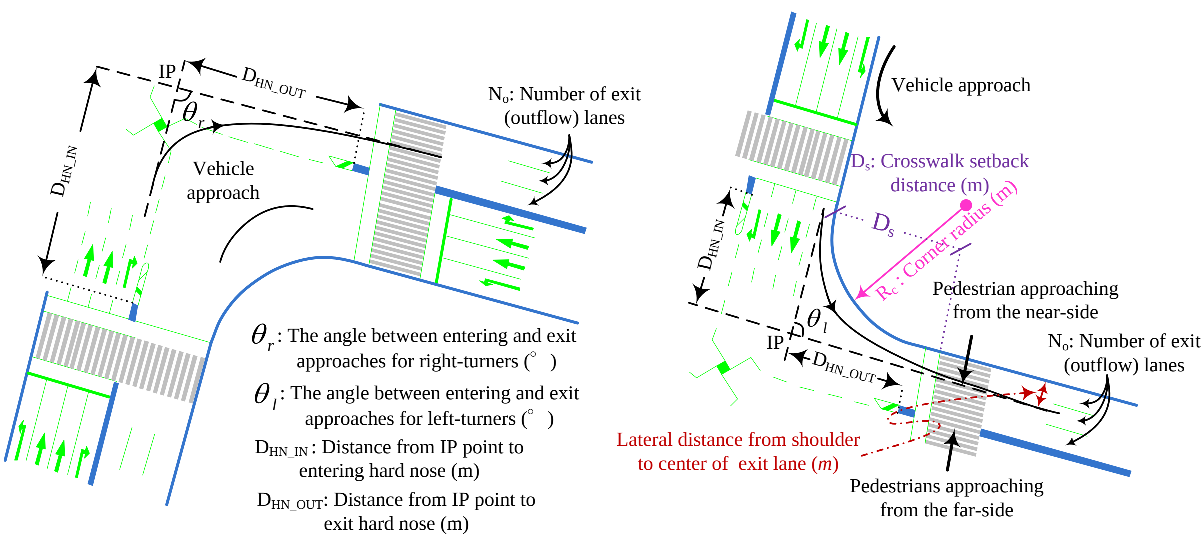


Figure 1 Definition of the parameters related to intersection layout

Table 3 Traffic volumes of measured intersection approaches

| Intersection name | Approach | Turning vehicle demand (veh./h) | | Pedestrian demand (ped./h) | Bicycles demand (byc./h) | Pedestrian demand (ped./h) | Bicycles demand (byc./h) |
|---|---|---|---|---|---|---|---|
| | | Left | Right | Entering from near-side | | Entering from far-side | |
| Suemori-dori 2 | East | 312 | – | 28 | 60 | 28 | 28 |
| | West | 204 | 112 | 16 | 32 | 64 | 52 |
| | North | 304 | 136 | 8 | 32 | 12 | 36 |
| | South | – | 240 | – | –- | – | – |
| Chikatetsu Horita | East | 84 | – | 20 | 64 | 172 | 76 |
| | South | 28 | – | 20 | 36 | 128 | 36 |
| Taiko-dori 3 | West | 84 | 76 | – | – | – | – |
| | North | – | 76 | – | – | – | – |
| | South | 88 | – | 68 | 80 | 48 | 44 |
| Nishi-osu | West | 344 | – | 20 | 76 | 20 | 44 |
| | North | – | 120 | – | – | – | – |
| | East | – | 168 | – | – | – | – |
| Kawana | West | 208 | | 20 | 52 | 108 | 28 |
| | North | – | 268 | – | – | – | – |
| Imaike | North | 250 | – | 175 | 78 | 210 | 102 |
| Sunadabashi | West | – | 140 | – | – | – | – |
| | North | – | 400 | – | – | – | – |
| Sakurayama | South | – | 96 | – | – | – | – |
| Atsuta Shrine South | North | – | 84 | – | – | – | – |

**Trajectory Tracking**

Vehicle trajectories which include the positions and timings are extracted from video data by using video image processing system TrafficAnalyzer (Suzuki and Nakamura, 2006). The positions of each vehicle were extracted every 0.5 seconds and then their video coordinates are converted to the global coordinates by projective transformation. The point where the right-rear wheel is touching the ground is the reference observation point for all vehicles. All video observations were done from high buildings around the intersections, thus for all video tapes, the observation angle is large. This allows us to track the right rear wheel of all turning vehicles without facing any problems. By considering the dimension of each turning vehicle, the observed path based on the right-rear wheel is transformed to the path which corresponds to the center-front of the vehicle. The transformed paths are smoothened by Kalman smoothing method.

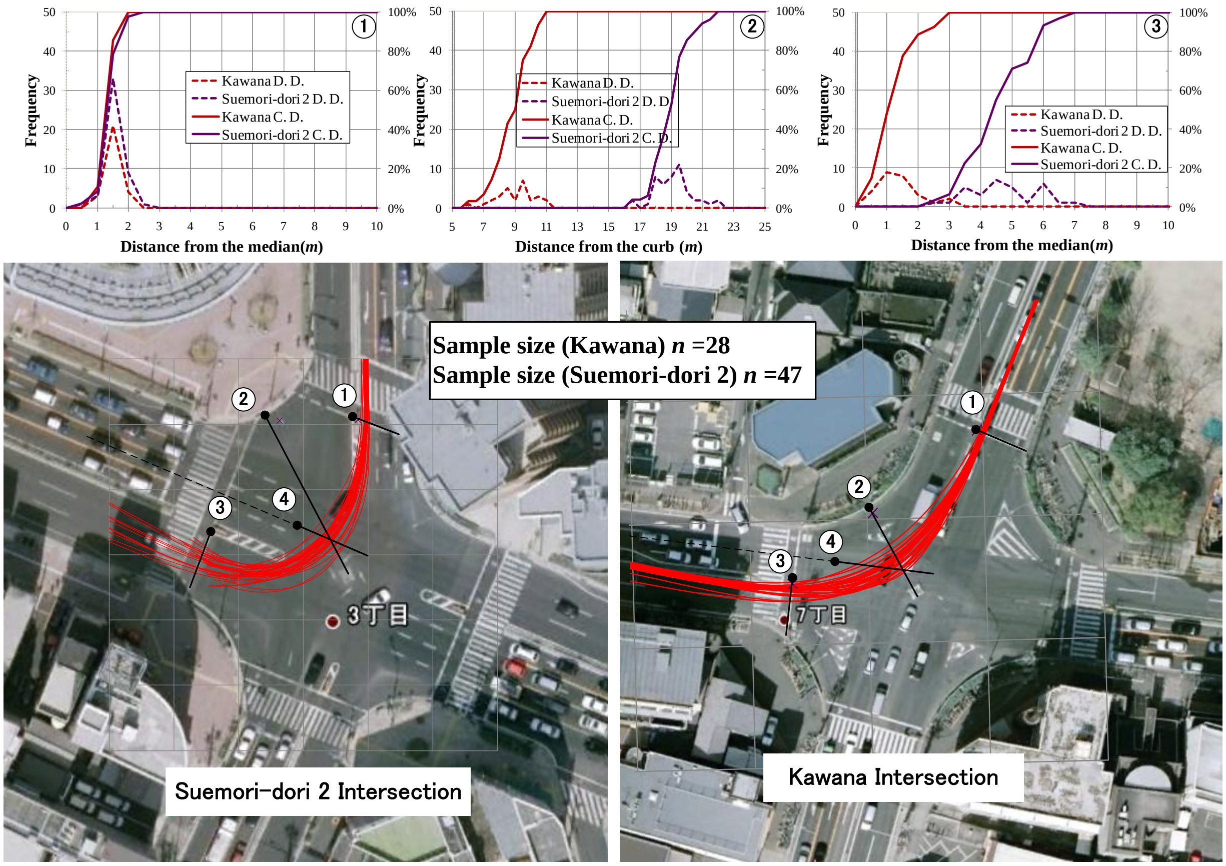


Figure 2 Paths of right-turning vehicles at the north approaches of Suemori-dori 2 Intersection and Kawana Intersection

## DATA ANALYSIS ON PATHS OF TURNING VEHICLES

There are several factors that might affect the variations in the paths of turning vehicles. According to the observations, turning angle (angle between entering and exit approaches), corner radius, number of exit lanes, vehicle type and approaching speed are the most significant factors that affect left-turning vehicle paths as discussed by Asano et al. (2011). Regarding right-turning vehicles, observations revealed that turning angle, the distances from the center of the intersection to the entering and to the exit hard noses (Figure 1), number of exit lanes and approaching speed are the most significant parameters on the distribution of vehicle paths.

The effect of turning angle on driver behavior while turning is demonstrated though Figure 2 in which the paths of right-turning vehicles at the north approach of Suemori-dori 2 Intersection and Kawana Intersection are compared. The lateral trajectory density distribution (D.D.) and the lateral cumulative distribution (C.D.) at three cross-sections along the turning paths are also presented. The density and cumulative distributions are drawn in an interval of 0.5m starting from the corner curb of the intersection. It is clear that the right-turning vehicle paths of at cross-section 2 and 3 are significantly less distributed at Kawana Intersection compared to Suemori-dori 2 Intersection (at 95% significance level). This can be referred to the sharp turning angle

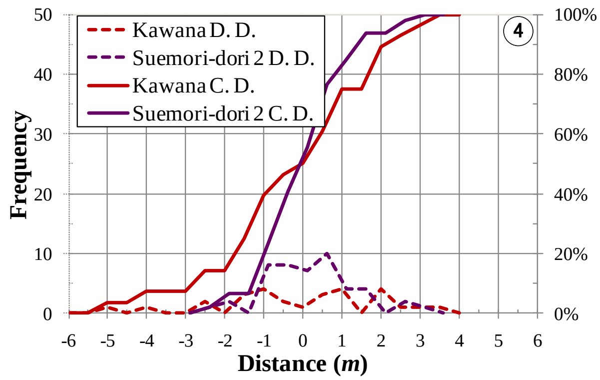


Figure 3 The distribution of conflict points between right-turners from the North approaches of Suemori-dori 2 Intersection and Kawana Intersection and crossing through traffic

from the north approach of Suemori-dori 2 Intersection which leads to a wider range of vehicle paths. Furthermore, the west approach of Suemori-dori 2 Intersection has 3 exit lanes while the west approach of Kawana Intersection has two only. More exit lanes give drivers higher degree of freedom and more choices which is reflected in wider trajectory distributions.

Another possible factor that might affect driver behavior while turning is the existence of pedestrians. However, Asano et al. (2011) found that the difference in the trajectories of the vehicles that faced and did not face pedestrians or cyclists, is not statistically significant at 95% confidence interval.

According to the previous analysis, it is concluded that there are significant variations in the turning vehicle trajectories dependent on several factors. Furthermore, after excluding the effects of the factors discussed above, there are still significant variations in turning vehicle trajectories which can be referred to some other external factors that affect driver behavior. It is important to mention here that available data is not enough to investigate the effect of vehicle type on the paths of right-turning vehicles.

The variations in vehicle paths significantly affect the positions of conflicts with other users. For better understanding of this relationship, the distribution of the conflict points between right-turning vehicles and crossing through traffic entering in the beginning of the next phase is illustrated in Figure 3. For that, it is assumed that paths of crossing through traffic is in the middle of the approach lane and do not change their direction inside the intersections. Therefore it is assumed that cross-section 4 in Figure 2 represents the average path of entering through traffic. This means that all conflict points will be located along this cross-section. Figure 3 shows the observed distributions of conflicts at Kawana and Suemori-dori Intersections. The horizontal axis refers to the position along the cross-section 4 in which the origin is the point where 50 percentile of the conflict points along the axis is measured. Figure 3 clearly shows that the conflict points are widely distributed at both intersections. Meanwhile Kawana Intersection has a significantly wider distribution compared to Suemori-dori Inetersection. Kawana Intersection has a very long distance from the center of the intersection to the entering hard nose (almost 35*m*). Such a long distance encourages drivers to start turning earlier which leads to a wider distribution of conflict points. These observed wide distributions of conflict points might impact on the occurrence probability of hazardous conditions.

## STRUCTURE OF TRAJECTORY MODEL

The objective of this paper is to model the distribution of turning vehicle paths as a function of intersection geometries and vehicle types. The model is intended to be incorporated into a microscopic simulation model for safety evaluation so that it can represent how vehicle positions vary according to the intersection geometries. Generally, the modeling methodology can be divided into the two consecutive steps as follows:

1) Individual vehicle path approximation, and
2) Modeling the variations in paths.

In general, the path of a turning vehicle is defined as a set of vehicle positions at each moment while turning. Therefore, modeling vehicle paths means representing vehicle positions sequentially as time proceeds. Instead of sequential representation of vehicle positions, this paper approximates the whole turning movements as a combination of straight lines, Euler spiral curves and circular curves as shown in Figure 4. The advantage of this approximation method is that the complicated shape of the paths can be expressed by few parameters; start and end points of the turning path, circular curve radius and Euler spiral parameter.

Vehicle paths vary as discussed in the previous section. Estimating the distribution of paths is also important for safety evaluation. In this study, this distribution is assumed to be dependent on several representative parameters which are normally distributed.

### Individual vehicle path approximation

<u>Curvature Calculation</u>

It is assumed that vehicle paths consist of small portions of curves with different curvatures. $P_i(t)$ is assumed as position of vehicle $i$ at time $t$. Furthermore, $O_i(t)$ is defined as the crossing point between perpendicular bisector of positions $P_i(t\text{-}\Delta t)$ and $P_i(t)$ with that of positions $P_i(t)$ and $P_i(t+\Delta t)$ as illustrated in Figure 4a). Curve radius $R_i(t)$ at position $P_i(t)$ represents the radius of a circle, which its center is at $O_i(t)$ and passes through the positions $P_i(t\text{-}\Delta t)$, $P_i(t)$ and $P_i(t+\Delta t)$. Observation time interval $\Delta t$ is set as 0.5 seconds. Curvature $\kappa_i(t)$ is the reciprocal of $R_i(t)$ $(=1/R_i(t))$. Figure 4b) shows an example of the observed curvatures of left and right-turning vehicle paths at the North approach of Suemori-dori 2 Intersection. Horizontal axis of Figure 4b) is normalized so that the position of stop line in Figure 4b) is corresponding to 0 and the position of the end of path measurement (slightly downstream of the exit crosswalk) corresponds to 1. Most of the curvature profiles in Figure 4b) start from 0, and then monotonously increase until the middle of the curve where it starts decreasing to 0 again. This characteristic implies that turning-vehicle paths can be represented by modeling the change in the curvatures.

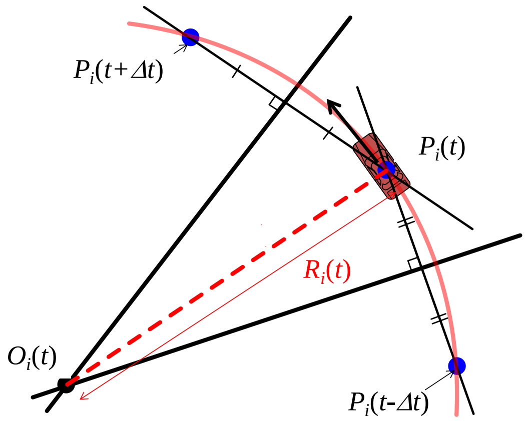


a) Curvature calculation

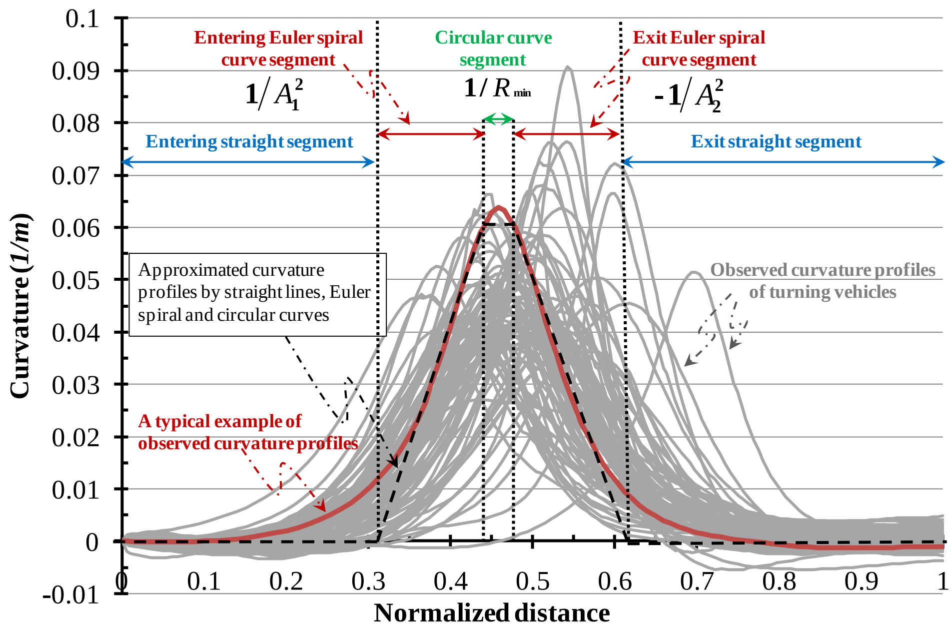


b) Observed and approximated curvature profiles at Suemori-dori2 intersection (North approach)

Figure 4 The curvature profile of turning vehicles and its parameters

<u>Trajectory Elements</u>

For modeling the change in the curvatures, three types of segments are used; straight lines, circular curves and Euler spiral curves as shown in Figure 5. This section explains the features of these curves and their curvature.

Basically, the curvature of any straight lines is 0 while circular curves have constant curvature. Euler spiral curves are generally installed in road alignment as transition segments between straight and circular curve segments in order not to force drivers to steer suddenly when entering the circular curve. Basic formula of Euler spiral curves is shown below.

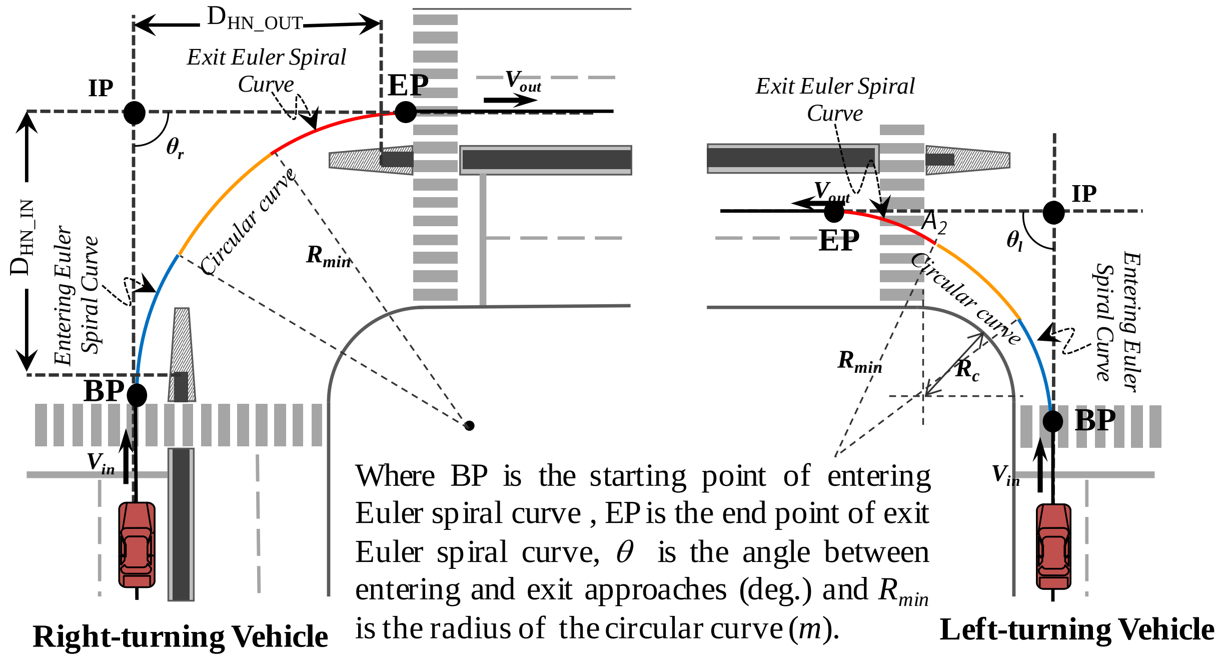


Figure 5 Trajectory approximation of left-turning and left-turning vehicles using Circular and Euler spiral curves

$$R_s L_s = A^2 \tag{1}$$

where $R_s$ is the radius of the spiral curve at the end point (the point where it is connected to the circular curve in this study), $L_s$ is distance from the spiral starting point and $A$ is parameter of the Euler spiral curve to be estimated. Equation (1) can be rewritten as follows:

$$\frac{1}{R_s} = \frac{1}{A^2} L_s \tag{2}$$

Equation (2) shows that the curvature of an Euler spiral curve is a linear function of $L_s$, with a gradient of $1/A^2$ .

Path Approximation

According to the curvature profiles in Figure 4b), it is reasonable to approximate a curvature profile in a polygonal line, which is a combination of straight, Euler spiral and circular curve segments. This polygonal line starts from a straight segment and then moves to an Euler curve segment with a linear curvature of $1/A_1{}^2$ gradient. This Euler curve is followed by circular curve segment with a constant curvature $1/R_{\min}{}^2$ , then an Euler curve segment which has linear curvature with a gradient of $-1/A_2{}^2$ and finally it comes back to a straight segment. These curves are defined as entering straight segment, entering Euler spiral curve segment, circular

Table 4 Parameters of trajectory approximation (right-turning vehicles)

| Intersection | | Exit lane* | $A_1$ | | $R_{min}$ | | $A_2$ | | Number of samples |
|---|---|---|---|---|---|---|---|---|---|
| name | Approach | | Average (m) | Standard deviation (m) | Average (m) | Standard deviation (m) | Average (m) | Standard deviation (m) | |
| Suemori-dori 2 | West | 1 | 21.45 | 1.39 | 19.12 | 1.34 | 21.75 | 1.28 | 4 |
| | | 2 | 19.10 | 1.85 | 17.34 | 3.09 | 19.33 | 2.43 | 6 |
| | North | 2 | 21.68 | 1.92 | 1.889 | 0.73 | 18.99 | 1.76 | 6 |
| | | 3 | 20.41 | − | 12.42 | − | 14.70 | − | 1 |
| | South | 1 | 23.55 | 2.94 | 21.39 | 6.10 | 25.16 | 5.53 | 2 |
| | | 2 | 22.60 | 1.37 | 18.09 | 2.04 | 21.16 | 1.52 | 3 |
| Sunadabashi (West) | West | 1 | 24.35 | − | 21.24 | − | 20.72 | − | 1 |
| | | 2 | 20.34 | 2.65 | 18.59 | 2.73 | 19.30 | 2.98 | 11 |
| | North | 1 | 18.53 | 2.01 | 16.78 | 1.66 | 19.84 | 1.44 | 5 |
| Nishi-osu | North | 2 | 22.92 | 2.67 | 19.35 | 3.27 | 23.63 | 3.23 | 10 |
| | | 3 | 21.77 | 3.00 | 20.26 | 1.98 | 27.12 | 3.44 | 5 |
| | South | 2 | 17.96 | 1.99 | 19.63 | 3.23 | 27.06 | 5.84 | 2 |
| | | 3 | 19.31 | − | 17.91 | − | 31.17 | − | 1 |
| | | 4 | 22.23 | 2.18 | 16.61 | 2.46 | 20.30 | 1.66 | 2 |
| | | 5 | 25.18 | − | 15.60 | − | 19.65 | − | 1 |
| Kawana | North | 2 | 28.26 | 4.85 | 26.59 | 6.01 | 27.68 | 3.89 | 13 |
| Sakurayama | South | 1 | 24.52 | 0.69 | 22.18 | 1.56 | 25.80 | 2.50 | 3 |
| | | 2 | 22.58 | 3.36 | 23.71 | 4.43 | 20.85 | 5.23 | 3 |
| Atsuta Shrine South | North | 1 | 24.22 | − | 24.45 | − | 25.70 | − | 1 |
| | | 2 | 21.30 | 0.91 | 20.59 | 2.20 | 30.38 | 5.35 | 3 |
| | | 3 | 19.76 | 2.00 | 16.89 | 1.09 | 27.86 | 2.10 | 5 |
| | | 4 | 15.39 | − | 14.79 | − | 26.05 | − | 1 |
| Taiko-dori 3 | West | 2 | 21.84 | 2.64 | 17.06 | 2.35 | 20.73 | 3.35 | 17 |
| | North | 1 | 24.43 | 1.30 | 24.01 | 0.82 | 25.75 | 0.03 | 2 |
| | | 2 | 23.72 | 2.44 | 20.55 | 3.26 | 22.71 | 3.29 | 9 |

* Exit lane is numbered from the median (center) to the shoulder.

curve segment, exit Euler spiral curve segment and exit straight segment, respectively. This polygonal line can be uniquely determined by defining 5 parameters, $A_1$, $A_2$, $R_{min}$, starting point of entering Euler spiral curve BP and end point of exit Euler spiral curve EP as shown in Figure 5. By applying the dynamic programming, these parameters for each vehicle trajectory are estimated by minimizing the error between the polygonal line and the measured curvature profile.

To provide a better insight on the path approximation, Table 4 shows the utilized data in the path model estimation for right-turning vehicles. The average and standard deviation of estimated parameter $A_1$, $A_2$ and $R_{min}$ are shown in Table 4. The sample size in Table 4 is different from that in Figure 2, since only leading vehicles were considered and the following vehicles were excluded in the modeling.

Table 5 Results of estimated Euler spiral parameters

| Explanatory variables | | Parameter of entering Euler spiral curve $A_1(m)$ Coefficients (t-values) | | Parameter of exit Euler spiral curve $A_2$ $(m)$ Coefficients (t-values) | |
|---|---|---|---|---|---|
| | | Left-turning | Right-turning | Left-turning | Right-turning |
| Const. | | -1.65(-1.85) | -8.65(-3.33) | 2.33(2.83) | 3.63(1.64) |
| Corner radius $R_c$ $(m)$ | | 0.334(8.73) | — | 0.335(7.52) | — |
| The angle between entering and exit approaches θ (deg.) | | 0.0404(3.61) | — | — | — |
| Heavy vehicle dummy (heavy vehicle:1, passenger car: 0) | | — | — | 2.05(2.89) | — |
| Lateral distance from shoulder to center of exit lane $(m)$ | | 0.461(7.70) | — | 1.04(15.2) | — |
| Distance from IP point to hard nose $(m)$* | $D_{HN\_IN}$ | — | 0.172(6.9) | — | — |
| | $D_{HN\_OUT}$ | — | — | — | 0.241(4.84) |
| Minimum speed $V_{min}(km/h)$ | | 0.369(9.04) | 0.294(4.48) | 0.268(6.88) | 0.287(3.05) |
| Sample Size | | 238 | 117 | 238 | 117 |
| Modified $R^2$ | | 0.772 | 0.663 | 0.774 | 0.424 |

* Refer to Figure 5.

To reproduce vehicle paths, the lengths of Euler spiral and circular curve segments are uniquely calculated by the input variables $A_1$, $A_2$, $R_{min}$ and the angle between entering and exit approaches $\theta$ (Crothoid Pocketboo0k, 2001). In order to fix the global position of the curves, the global position of IP is required. IP is defined as the crossing point between the extended lines of the entering and the exit straight segments as shown in Figure 5.

**Modeling the variations in paths**

In this section, the effects of intersection geometry, vehicle speed and vehicle type on the distribution of approximated paths are modeled. The explanatory variables are vehicle approaching speed, minimum speed $V_{min}$ and the elements of intersection geometry such as intersection angle and corner radius. Output variables are the distribution of $A_1$, $A_2$ and $R_{min}$. The entering and exit Euler spiral curves' parameters $A_1$ and $A_2$ are estimated by multiple regression models as shown in Table 5.

For left turning vehicles, the estimated path parameters $A_1$, $A_2$ and $R_{min}$ are dependent on intersection geometry as shown in Table 5 and Table 6. However for right-turning vehicles, it was found that the effect of intersection geometry is insignificant on the entering and exit Euler spiral curves' parameters $A_1$ and $A_2$ except the distance from IP to the entering and exit median hard nose ($D_{HN\_IN}$ and $D_{HN\_OUT}$) which has significant impact.

The radius of the circular curve $R_{min}$ is estimated by assuming normal distribution as shown in Equation (3).

Table 6 Results of estimated minimum radius and minimum speed

| | Explanatory variables * | Radii of circular curve $R_{min}$ (*m*) Coefficients (t-values) | | Minimum speed $V_{min}$ (*km/h*) Coefficients (t-values) | |
|---|---|---|---|---|---|
| | | Left-turning | Right-turning | Left-turning | Right-turning |
| Average $\mu$ | Const. | -6.46(-6.31) | 1.862(0.67) | -1.08(-0.68) | 4.49(2.62) |
| | Corner radius $R_c$ (*m*) | 0.390(12.9) | — | 0.218(3.68) | — |
| | The angle between entering and exit approaches θ (deg.) | 0.127(13.1) | 0.062(2.36) | 0.139(8.12) | 0.072(5.57) |
| | Heavy vehicle dummy (heavy vehicle:1, passenger car: 0) | — | — | -1.787(-1.6) | — |
| | Lateral distance from shoulder to center of exit lane (*m*) | 0.862(16.8) | — | 0.838(8.44) | — |
| | Distance from IP point to hard nose (*m*)*: $D_{HN\_IN}$ | — | — | — | 0.0092(4.5) |
| | Distance from IP point to hard nose (*m*)*: $D_{HN\_OUT}$ | — | — | — | 0.105(3.17) |
| | Minimum between $D_{HN\_IN}$ and $D_{HN\_OUT}$ | — | 0.126(3.2) | — | — |
| | Approaching speed $V_{in}$(*km/h*) | | | 0.091(2.99) | 0.380(13.1) |
| | Minimum speed $V_{min}$(*km/h*) | — | 0.364(4.4) | — | — |
| Standard deviation σ | Const. | -2.86(-3.77) | 0.599(0.5) | 2.39(7.44) | 0.127(2.69) |
| | Corner radius $R_c$ (*m*) | 0.0624(3.09) | — | — | — |
| | The angle between entering and exit approaches θ (deg.) | 0.0363(4.95) | — | — | 1.71(4.57) |
| | Lateral distance from shoulder to center of exit lane (*m*) | 0.118(3.89) | — | 0.151(2.34) | — |
| | Minimum speed $V_{min}$(*km/h*) | — | 0.101(2.17) | — | — |
| Sample size | | 238 | 117 | 238 | 117 |

* All variables related to intersection geometry are shown in Figure 1.

$$
\begin{aligned}
&R_{\min} \sim N(\mu,\sigma) \\
&\quad \mu = f(x_1, x_2 \sim x_n) = \alpha_{1,1}x_1 + \alpha_{1,2}x_2 \sim \alpha_{1,n}x_n + \alpha_{1,n+1} \\
&\quad \sigma = f(x_1, x_2 \sim x_n) = \alpha_{2,1}x_1 + \alpha_{2,2}x_2 \sim \alpha_{2,n}x_n + \alpha_{2,n+1}
\end{aligned}
\tag{3}
$$

where $\mu$ is the mean of the normal distribution (*m*), $\sigma$ is the standard deviation of the normal distribution (*m*), $x_1$, …$x_n$ are independent variables, $\alpha_{1,1}$, …, $\alpha_{1,n}$, $\alpha_{2,1}$ and $\alpha_{2,n}$ are the model coefficients estimated by maximum likelihood method. The estimation results for left-turning and right-turning vehicles are shown in Table 6.

Vehicle minimum $V_{min}$ speed along the whole maneuver (leading vehicles only that did not face any pedestrian or cyclist) is used as one of the explanatory variables in modeling the parameters for the entering and the exit Euler spiral curves and in modeling the radius of the circular curve $R_{min}$ as well. Vehicle minimum speed $V_{min}$ is modeled by assuming normal distribution as shown in Equation (4).

$$V_{\min} \sim N(\mu,\sigma)$$
$$\mu = f(x_1, x_2 \sim x_n) = \beta_{1,1}x_1 + \beta_{1,2}x_2 \sim \beta_{1,n}x_n + \beta_{1,n+1} \quad (4)$$
$$\sigma = f(x_1, x_2 \sim x_n) = \beta_{2,1}x_1 + \beta_{2,2}x_2 \sim \beta_{2,n}x_n + \beta_{2,n+1}$$

where $\mu$ is the mean of the normal distribution (*m*), $\sigma$ is the standard deviation of the normal distribution (*m*), $x_1$, …$x_n$ are independent variables, $\beta_{1,1}$, …, $\beta_{1,n}$, $\beta_{2,1}$ and $\beta_{2,n}$ are the model coefficients estimated by maximum likelihood method. The estimation results of $V_{min}$ for left-turning and right-turning vehicles are shown in Table 6. The minimum speed $V_{min}$ of turning vehicles along the turning path is dependent on approaching speed $V_{in}$ as shown in Table 6 which is quite rational. Turning vehicles with high running speeds approaching the intersection will reach higher minimum speeds compared to other vehicles that are approaching the intersection with low running speeds.

In reality, vehicle path is not independent from its speed. This correlation between vehicle path and speed is empirically proven in this study. Vehicle path is affected by the entering speed of the vehicle $V_{in}$ which defines with intersection geometry the minimum speed reached along the turning path $V_{min}$. This phenomenon is reflected in the developed empirical models as shown in Table 5 and Table 6.

So far, since the available data of right-turning heavy vehicles is not sufficient to reflect the effect of vehicle type, all developed models for right-turning vehicle paths do not consider vehicle type.

## COMPARISON BETWEEN ESTIMATED AND OBSERVED PATHS

Although the estimated parameters are well-fitted, each variable just explains a part from the whole path. For validation, generated distributions are compared with the actual distributions.

Figure 6 compares the estimated and observed path distributions of left-turning passenger cars at west approach of Nishi-osu Intersection. IP is set for path generation by assuming that the entering and exit straight segments are located at the midpoint of each lane. Observed lane usage ratio of exit lanes is used in the developed path model to generate turning vehicle paths. Monte-Carlo simulation with 1000 trials is conducted to generate these path distributions.

Red-colored numbers of each graph in Figure 6 correspond to the cross-sections defined along vehicle path. The estimated paths clearly fit well especially the paths before reaching the exit crosswalks. The shape of the estimated distribution at cross-section 3 tends to be stepwise since the exit straight segments are located at the center of traffic lanes. However in reality, the positions of the exit straight segments may also vary laterally inside each lane.

Figure 7 compares the estimated and observed path distributions of right-turning passenger cars from the North approach of Nishi-osu Intersection. The results are very similar to that of left-turning vehicles. The estimated path distributions at cross-section 1 and 2 are not significantly different (95% confidence level) from the observed ones while at cross-section 3 they are significantly different. This difference is referred to the assumed exit positions which are located in the middle point of each exit lane.

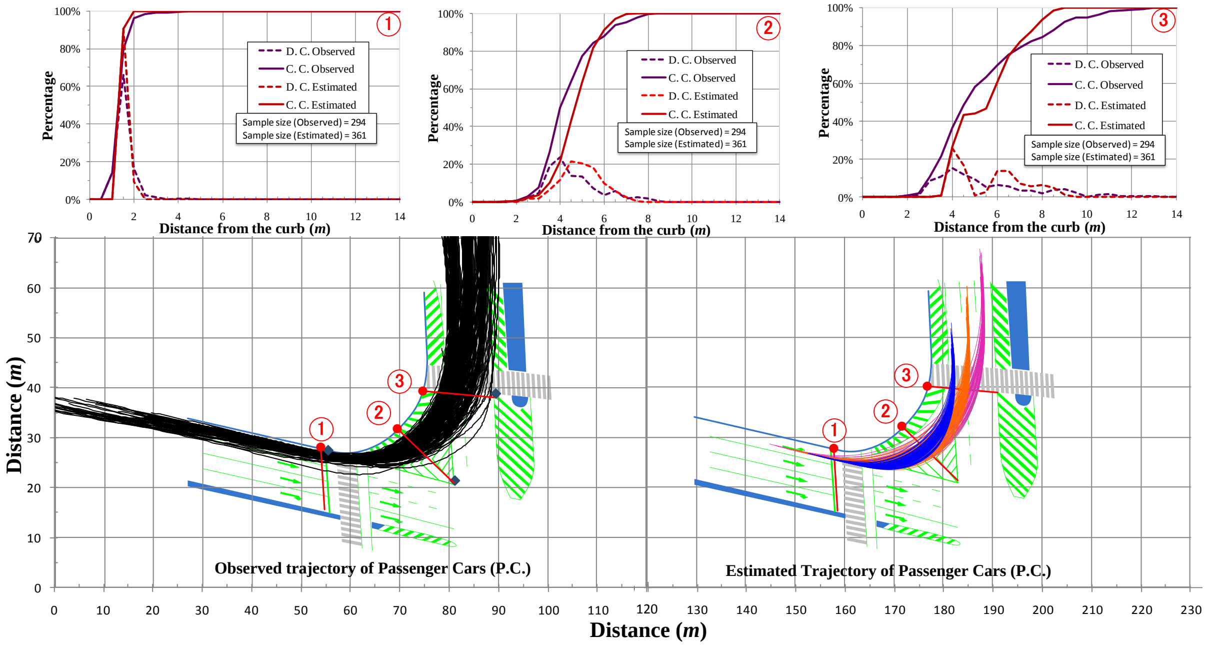


Figure 6 Comparison between observed and estimated paths of left-turning passenger cars at the West approach of Nishi-osu Intersection

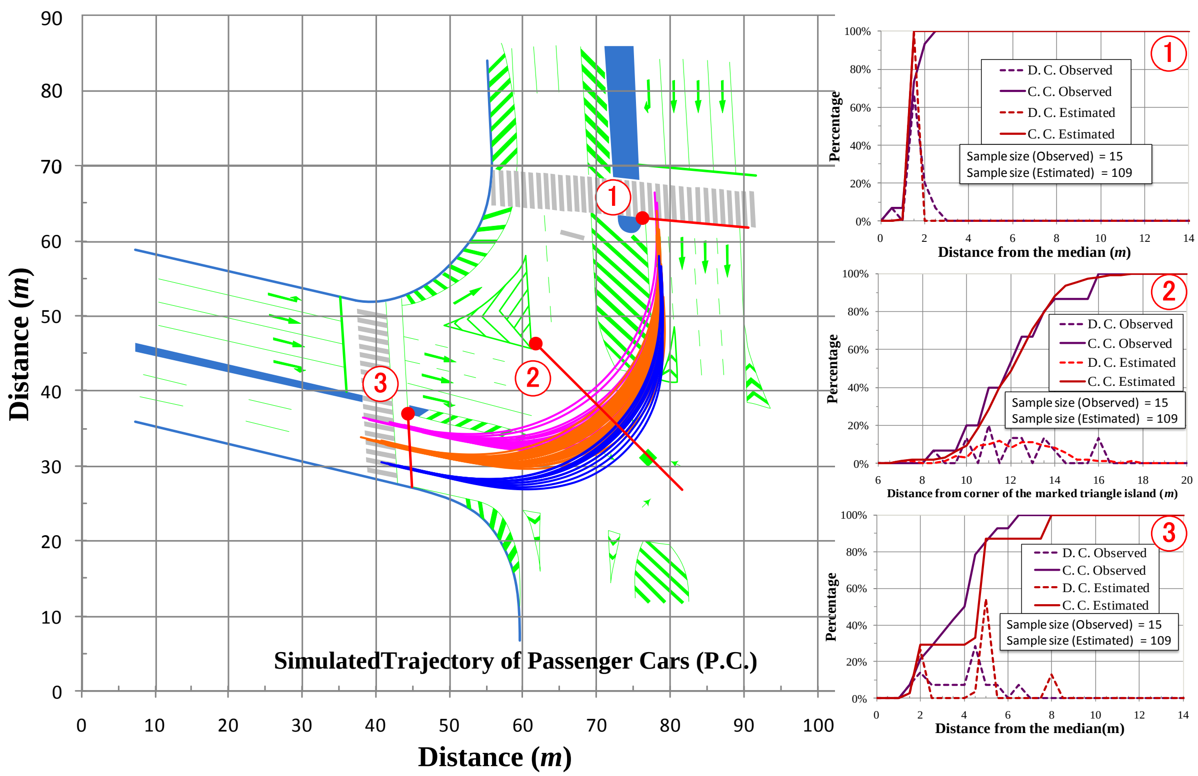


Figure 7 Comparison between observed and estimated paths of right-turning vehicles at the North approach of Nishi-osu Intersection

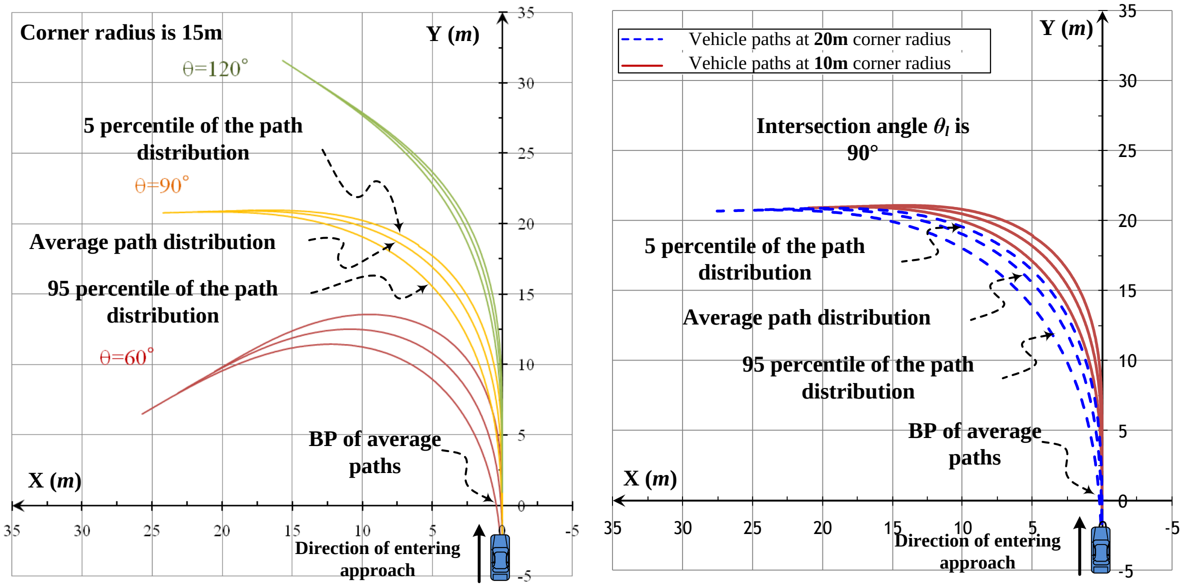


a) Different angles between the entering and exit approaches

b) Different corner radii

Figure 8 Sensitivity of left-turning vehicle paths to intersection geometric parameters

## SENSITIVITY ANALYSIS

The effect of intersection geometry on left-turning vehicle paths is demonstrated by using the developed models. Figure 8a) shows estimated path distributions at hypothetical intersections with corner radius of 15*m*. Left-turning vehicle paths are estimated at three different intersection angles, 60, 90 and 120 degrees. Origin point of X axis is assumed as the entering point of the intersection. Furthermore, it is assumed that all hypothetical intersections have one exit lane. The lateral distance between the center of the vehicle and the curb is set as 1.5m. The results show that the approach with smaller angle tends to have larger path variations. This can be referred to the ability of left-turning drivers to maintain their higher speeds at larger angle approaches while in smaller angles they need to reduce their speed which reflects directly on the turning radius and further the whole maneuver. It is rational to conclude that the probability that drivers might change their maneuver (speed and position) becomes smaller if intersection angle is large and vehicle speed is high.

Figure 8b) shows estimated path distributions at two hypothetical intersections with corner radius of 10m and 20m while intersection angle is kept the same (90 degrees) for both intersections. It is clear that intersection radius significantly affects the distribution of vehicle paths. Larger corner radii will result in longer turning maneuvers as shown in Figure 8b).

To illustrate the effect of the angle between entering and exit approaches $\theta_r$ on the variation of right-turning vehicle paths, Figure 9 is presented. It is assumed that all right-turning vehicles will exit in one lane which is the median lane. It concluded that as the angle $\theta_r$ increases, vehicle

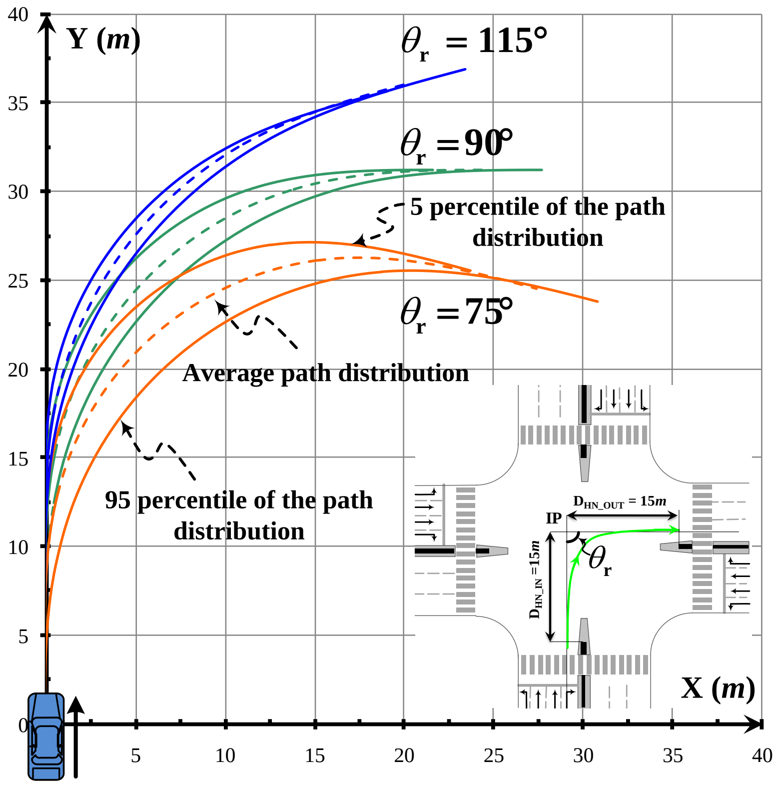


Figure 9 Sensitivity of right-turning vehicle paths to intersection geometric parameters

paths become less distributed. These results are rational since the possibility that drivers can maintain their speed becomes higher as the angle $\theta_r$ increases which means that the effect will become milder. This is in accordance with the results of left-turning vehicles.

## CONCLUSIONS

In this paper, the trajectory distribution of turning vehicles is analyzed and modeled as a function of intersection geometry, vehicle type and speed. According to the empirical data analysis, it is concluded that the path distribution of left-turning vehicles is mainly dependent on intersection angle, corner radius, number of exit lanes, vehicle type and approaching speed. Meanwhile the path distribution of right-turning vehicles is dependent on the angle between entering and exit approaches, the positions of the entering and the exit hard noses of the median (Figure 1), number of exit lanes and vehicle approaching speed. Furthermore, this study proved that the variations in vehicle paths significantly affect the distribution of conflict points which implies that the path distribution may strongly impact on the occurrence probability of severe conflicts.

A unique model which can reflect the variations in turning vehicle paths is proposed. By comparing estimated and observed paths, it is concluded that the developed model can reasonably represent the effect of intersection geometry not only on average vehicle trajectories but also on their distribution. This quantitative representation of detailed microscopic behavior can be used to predict the changes in vehicle maneuver as a result of any improvements on intersection layout. Furthermore, the proposed model joined with other behavioral models can be utilized to evaluate intersection safety stochastically.

However, the proposed trajectory model still has several limitations. The exit positions are assumed as input to the trajectory model. Since exit positions are widely distributed as shown in Figure 2, incorporating lane choice model in the proposed methodology is necessary to provide a complete procedure to reproduce the spatial maneuver of turning vehicles. Furthermore, number of turning lanes and turning lane width are not considered in the developed methodology since available data does not include various sites with different numbers of turning lanes and widths.

It is planned to utilize the developed turning vehicle path model in a microscopic simulation tool for the safety evaluation of signalized intersections. However a trajectory model only will not be sufficient, thus a probabilistic speed profile model, which considers the yielding behavior as a result of intersection geometry and the interaction with other users, is necessary to provide a successful presentation of the left-turning vehicle behavior in a microscopic simulation environment.

**ACKNOWLEDGEMENTS**

Authors are very grateful to Takata Foundation and Japan Society for the Promotion of Science (JSPS) for supporting this research.

**REFERENCES**

AASHTO. (2004). A Policy on Geometric Design of Highways and Streets. USA.

Asano, M., Alhajyaseen, W. K. M., Suzuki, K. and Nakamura, H.: Modeling Variation in the Trajectory of Left-Turning Vehicles Considering Intersection Geometry, 90th TRB Annual Meeting, 17 pages, 2011.

Decabooter, P. H. and Solberg, C. E. (1988). Designated Highway System Truck Operation Study, “Geometric Considerations”. Proceedings of the 67th Annual Meeting of the Transportation Research Board, Washington D. C., USA.

Japan Road Association. (2001). Crothoid Pocketbook, Tokyo, Japan. (in Japanese)

Read, M. P. (2008). Intersection Kinematics: A Pilot Study of Driver Turning Behavior with Application to Pedestrian Obscuration by A-Pillars. Report No. UMTRI-2008-54. Transportation Research Institute, The University of Michigan, USA.

Stover, V. G. (2008). Issues Relating to the Geometric Design of Intersections. Proceedings of the 8th International Conference in ACCESS Management. Baltimore, MD, USA.

Stover, V. G. and Koepke, F. J. (2002). Transportation and Land Development, Institute of Transportation Engineers, 2nd edition.

Suzuki, K. and Nakamura, H. (2006). TrafficAnalyzer - The Integrated Video Image Processing System for Traffic Flow Analysis. Proceedings of the 13th World Congress on Intelligent Transportation Systems, 8 pages in CD-ROM, London.